THE ASTROPHYSICAL JOURNAL, 309:674–681, 1986 October 15

EFFECTS OF HIGH-ENERGY NEUTRINO PRODUCTION AND INTERACTIONS ON STARS IN CLOSE X-RAY BINARIES

T. K. GAISSER
Bartol Research Foundation of the Franklin Institute

AND

F. W. STECKER, A. K. HARDING, AND J. J. BARNARD[1]
Laboratory for High Energy Astrophysics, NASA Goddard Space Flight Center
Received 1986 February 18; accepted 1986 April 2

ABSTRACT

We discuss limits that may be placed on binary systems in which a compact partner is a strong source of high-energy particles that produce photons, neutrinos, and other secondary particles in the companion star. The highest energy neutrinos are absorbed deep in the companion and the associated energy deposition may be large enough to effect its structure or lead to its ultimate disruption. We evaluate this neutrino heating, starting with a detailed numerical calculation of the hadronic cascade induced in the atmosphere of the companion star. For some theoretical models, the resulting energy deposition from neutrino absorption may be so great as to disrupt the companion star over a time scale of 10^4–10^5 yr. Even if the energy deposition is smaller, it may still be high enough to alter the system substantially, perhaps leading to quenching of high-energy signals from the source. Given the cosmic-ray luminosities required to produce the observed γ-rays from Cygnus X-3 and LMC X-4, such a situation may occur in these sources.

Subject headings: cosmic rays: general — neutrinos — stars: interiors — X-rays: binaries

I. INTRODUCTION

Reports of air showers with $E > 10^{15}$ eV from Cygnus X-3 (Samorski and Stamm 1983*a*; Lloyd-Evans *et al.* 1983; Kifune *et al.* 1985), LMC X-4 (Protheroe and Clay 1985), Vela X-1 (Protheroe, Clay, and Gerhardy 1984), and Hercules X-1 (Baltrusaitis *et al.* 1985) have been interpreted as requiring production of neutral secondaries by cosmic rays accelerated by the compact partner of these systems. If neutral pions are the source of photons that produce the observed air showers (Hillas 1984), then charged pions must also be produced, and they will give rise to neutrinos (Eichler 1978). There is a question as to whether the muon content of these showers is high, indicative of hadronically induced showers (Samorski and Stamm 1983*b*), or low, indicative of electromagnetically (photon) induced showers (Kifune *et al.* 1985). It has been proposed (Vestrand and Eichler 1979, 1982; Berezinsky 1980; Hillas 1984) that the atmosphere of the companion star provides the grammage required to stop the accelerated particles and produce high-energy γ-rays. Reports of underground muons from secondary ultra–high-energy particles produced by Cygnus X-3 (Marshak *et al.* 1985; Battistoni *et al.* 1985; Bayere *et al.* 1985), although in question (Chudakov 1985), have led to speculations of exotic particles and production mechanisms (Stenger 1985; Baym *et al.* 1985; see, however, Barnhill *et al.* 1985; Berezinsky 1985; Mackenzie and Thacker 1985; Mohapatra, Nussinov, and Vallé 1985), which would also be accompanied by charged pion-neutrino production, so that neutrino beams would also arise in these scenarios.

In this paper we address in more detail some questions first discussed by Stecker, Harding, and Barnard (1985; hereafter SHB) viz., what happens when the companion star acts as a beam dump for its compact partner which is a powerful primary cosmic-ray accelerator? What is the resulting neutrino flux and how much energy is absorbed? How does the system respond to rates of energy deposition which may be much greater than the stellar luminosity of the companion?

We first review the calculation of the hadronic cascade in the outer layers of the companion. This cascade ultimately gives rise to neutrinos and photons. We next calculate the rate of energy deposition in the companion by the cascade, with emphasis on the neutrinos which penetrate deeply into the star. We finally conclude with a discussion of the consequences of this energy deposition for the stability of the system.

II. NEUTRINO PRODUCTION

Hillas (1984) has calculated the electromagnetic cascade produced by collisions of the accelerated protons in a distribution of gas around the companion. He estimated that the observed air shower signal from Cygnus X-3 requires a cosmic-ray luminosity for the source of

$$L_{cr} \approx 5 \times 10^{39} \left(\frac{0.02}{D_\gamma}\right) \frac{\Delta\Omega}{4\pi} \left(\frac{d}{12\ \mathrm{kpc}}\right)^2 \mathrm{ergs\ s^{-1}}, \qquad (1)$$

where D_γ is the duty cycle for production of the photon signal, $\Delta\Omega$ is the solid angle into which the high-energy particles are beamed, and d is the distance from the observer to the source. The power for other sources may be similarly estimated from their observed signals, and these results are summarized in Table 1. An important point is that a photon spectrum with $dn_\gamma/dE \propto E^{-2}$, as observed, can be produced by a parent spectrum that is harder than E^{-2}, including a δ-function spectrum. The E^{-2} photon spectrum is then achieved by electromagnetic cascading, either in strong ambient magnetic fields or in the gas.

The starting point for a calculation of the hadronic cascade induced by the accelerated cosmic rays from the compact

[1] National Research Council Research Associate.

TABLE 1

ASPECT RATIO (a/R) AND ESTIMATED COSMIC-RAY LUMINOSITY FOR SEVERAL BINARY SYSTEMS

System	Binary Period[a] (days)	Companion Mass ($M_\odot$)[a]	a/R[b]	Distance[a] (kpc)	L_{cr}[c] (ergs s^{-1})
Cyg X-3	0.19	$\lesssim 4$[d]	~ 1.4	$\gtrsim 12$	$\sim 10^{39}$
Vela X-1	8.965	23	12	1.4(?)	$\sim 10^{37}$
LMC X-4	1.408	~ 19	3.5	50	$\sim 10^{41}$
Her X-1	1.7	2.4	6	4	$\sim 10^{38}$

[a] From Rappaport and Joss (1983, and references therein), except for Cygnus X-3.

[b] The ratio of separation to radius of companion star, a/R, is estimated from Kepler's third law, assuming the compact object to have mass 1.4 $M_\odot$. Here R is the radius of a zero-age main-sequence star of the given mass.

[c] L_{cr} is estimated as in eq. (1).

[d] Assuming the compact object to be a neutron star from recent evidence that it is a pulsar (Chadwick *et al.* 1985) and the companion star radius to be less than the orbital radius.

source is the assumed density profile of the target material in the companion star. For purposes of illustration we first consider a main-sequence star of $M = 2.8\ M_\odot$. It has the density distribution shown in Figure 1. The dashed line shows the accumulated grammage X (g cm^{-2}) along the stellar diameter. From the density distribution (initially assumed to be spherically symmetric) one can similarly obtain the accumulated depth as a function of distance along any chord through the star. The calculation consists of following the hadronic cascade along each chord and taking the appropriate angular average, which depends on the assumed binary separation, a, and the size R of the companion (see Fig. 2). This calculation has been done by Gaisser and Stanev (1985) for the above example, taking account of all the details of production and decay, interaction, and multiplication of secondaries along the cascade. It was assumed that the compact object emits accelerated cosmic-

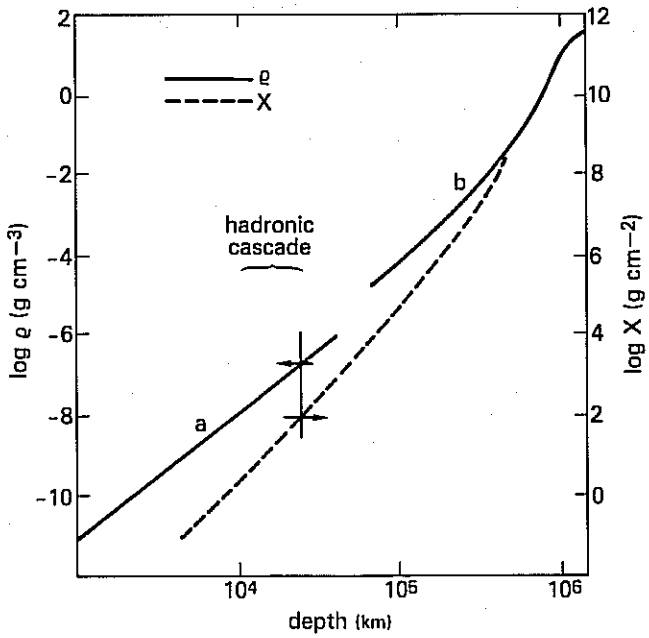

FIG. 1.—Density and grammage as a function of stellar depth for a 2.8 $M_\odot$ main-sequence star. Density curves (*a*) from stellar atmosphere model, (*b*) from stellar structure model.

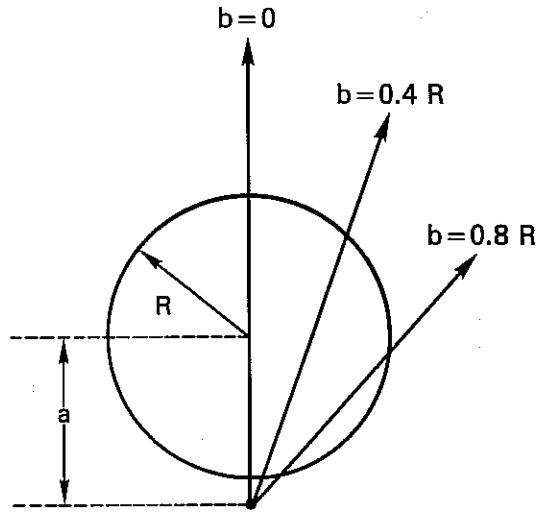

FIG. 2.—Geometry of the binary system with the compact object at a distance a from the center of the companion star of radius R, b being the impact parameter of the primary beam.

ray nucleons isotropically from a surface that is small compared to the distance from the source to the surface of the companion. Any other assumption simply requires straightforward modification of the geometry.

In order to understand qualitative aspects of the results it is helpful to see where in the companion star various processes occur. The hadronic cascade starts when $X < m_H/\sigma \approx 30$–$40$ g cm^{-2} in hydrogen for nucleon energies around 10^7 GeV (Baltrusaitis *et al.* 1984). By 10 interaction lengths it has saturated. This range of depths is marked on Figure 1, and it occurs in the outer part of the star at a density of $\sim 2 \times 10^{-7}$ g cm^{-3}. In contrast, the interaction length of multi-TeV neutrinos is of order 10^{11} g cm^{-2}, which occurs deep in the star at densities of order 1–10 g cm^{-3}. Thus, neutrino production and absorption are quite separate.

By comparing the charged pion interaction length, $m_H/\rho\sigma$, with its decay length, $\tau_\pi E_\pi/(m_\pi c) = 5.57 \times 10^6 E_\pi(\text{TeV})$ cm, we find a critical pion energy below which most charged pions decay into muons and neutrinos and above which they interact. This energy E_π^c corresponds to a critical neutrino energy $E_\nu^c \approx E_\pi^c/4$ given by (SHB)

$$E_\nu^c \approx 1.3 \times (10^{-6}/\rho)\ \text{TeV} \qquad (2)$$

at $X = m_H/\sigma$.

In fact this is a lower bound to the critical energy because the outer part of the star may likely have expanded in response to heating by the cascade (SHB, see also § III) and because for chords at impact parameter $b > 0$ the density at depth $X = m_H/\sigma$ will be lower than that along the diameter, which was used for the estimate in equation (2). In Figure 3 we show the neutrino flux produced by decay of charged pions and kaons in the outer layers of the star (Gaisser and Stanev 1985) for extreme cases, $b = 0$ and $b \approx R$. In the $b = 0$ case, the primary particles travel directly into the star, encountering greater densities than along any other chord. Consequently many of the pions interact before decaying, and the cascade is more extensive, resulting in a relatively soft spectrum. In the $b \approx R$ case, the particles encounter only the lower density of the stellar atmosphere. In this limit, all pions decay (with no cascading), resulting in a relatively hard spectrum. Spectra at other impact parameters are intermediate between these limits.

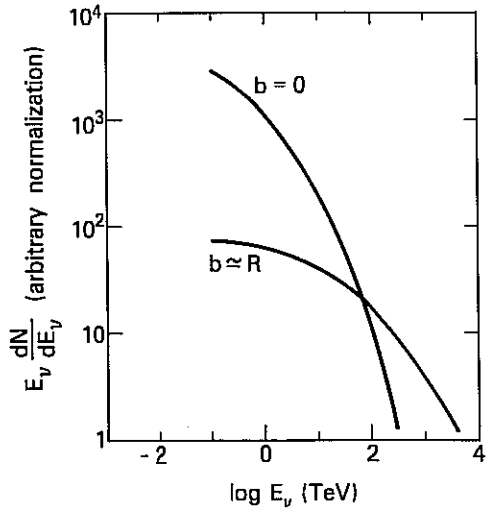

FIG. 3.—Neutrino spectrum at production, given a monoenergetic primary cosmic-ray spectrum of 10^{17} eV energy.

III. ELECTROMAGNETIC ENERGY DEPOSITION IN THE COMPANION STAR

The hadronic cascade in the outer regions of the star, in addition to producing the neutrino beam described above, will dissipate most of the rest of its energy in electromagnetic cascading induced by photons from decay of neutral pions. (A small fraction of the energy will be carried somewhat deeper by the muons from decay of charged pions.) Thus, more than half the energy of the cosmic rays hitting the companion will be dissipated at depths from several hundred to 1000 g cm^{-2}, characteristic of high-energy electromagnetic cascades. This will heat the atmosphere of the star and drive a stellar wind (SHB).

SHB also suggested that directly under the beam, ram pressure of the beam may compress the atmosphere. We show here, however, that, except for very unusual beam geometries (characterized by very small beam diameters relative to atmospheric scale heights), the atmospheric heating will drive a wind, even directly under the beam.

We may demonstrate this by examining the fluid equations governing a plane-parallel steady state atmosphere. Momentum conservation requires

$$\rho v \frac{dv}{dX} = -\frac{dP_{\rm gas}}{dX} - \frac{1}{3}\frac{dU}{dX} + \frac{\phi}{c}\left|\frac{dE}{dX}\right| + g\,, \tag{3}$$

where v is the fluid velocity, $P_{\rm gas}$ is the gas pressure, U is the radiation energy density (equal to 3 times the radiation pressure), ϕ is the incident cosmic-ray number flux, $|dE/dX|$ is the rate of energy loss per beam particle per unit grammage, g is the local gravitational acceleration in the stellar atmosphere, and X is the grammage through which the beam has passed, defined by

$$X = \int_z^\infty \rho dz\,, \tag{4}$$

where ρ is the mass density of the gas at height z in the atmosphere. The third term on the right-hand side of equation (3) represents the ram pressure of the beam on the stellar atmosphere. As well as being a source for momentum deposition, the rapidly thermalized beam energy is also a heat source which alters the outward energy flux, F:

$$\frac{dF}{dX} = -\phi\left|\frac{dE}{dX}\right| \tag{5}$$

If radiative transport is the main energy transport mechanism, then in the diffusion approximation,

$$\frac{dU}{dX} \approx \frac{3\kappa F}{c}\,, \tag{6}$$

where κ is the radiative opacity. Combining equations (3)–(6) yields

$$\rho v \frac{dv}{dX} = -\frac{dP_{\rm gas}}{dX} - \frac{\kappa F}{c} - \frac{1}{c}\frac{dF}{dX} + g\,. \tag{7}$$

In the case when radiative transport dominates (i.e., low beam energies) the outward flux increases from the original flux of the undisturbed star to the sum of the beam flux and original stellar flux as z increases (and X decreases). Thus dF/dX is negative, yielding a term having the effect of increasing the effective acceleration of gravity. However, the second term on the right-hand side of equation (7), representing the effect of the thermalized radiation pressure, is approximately κX_0 times larger than the third term, and of opposite sign, where X_0 is the typical grammage over which the energy from the beam is thermalized and κ is the opacity. Since $X_0 \approx 300$ g cm^{-2} and $\kappa \geq 0.4$ (equal to 0.4 for electron scattering), the third term is negligible compared to the second (the photon mean free path is small compared to the distance over which energy deposition occurs). Thus, radiation pressure from the thermalized beam will act to heat and expand the atmosphere, independent of the precise form of the energy deposition rate in the atmosphere.

This result has a simple physical interpretation. The beam flux, F_B, is transported into the star at a velocity $\sim c$, with a resulting beam energy density $U_B \approx F_B/c$. In steady state the cooling rate must equal the heating rate. The cooling rate for radiative transfer requires a temperature gradient, and from equation (6) requires a radiation density of order $\kappa X_0 F_B/c$ at depth X_0 in order to have an outward flux balancing the inward. Thus the effective diffusion "velocity" is $\sim c/(\kappa X_0) \ll c$. This result can be generalized to any energy transport mechanism, such as the advective transport of energy in a wind, or convective transport. For heating to balance cooling $cU_B \approx v_e U_I$, where U_I is the internal energy density and v_e is the outward flux divided by U_I and is the effective energy transport velocity. Since particles have finite cross sections and masses, and matter has finite opacity to photons, v_e is necessarily less than c. Thus U_I is greater than U_B, and so the ram pressure of the beam will be smaller than the thermal pressure of the heated atmosphere, and the atmosphere will be expanded relative to an undisturbed star (or flow outward for super-Eddington heating). This conclusion is based on a plane-parallel geometry. (If the beam width is much narrower than a scale height, sideways-directed flux can reduce the outward radiation pressure and increase the relative importance of the ram pressure.)

The implication of this discussion is that the density in the outer layers of the companion star, where the cascading and neutrino production occur, will be lower than in the undisturbed star. For example, in a stellar wind with constant velocity, the density falls off with the square of the radial distance.

Since $X = \int_r^\infty \rho dr \propto r^{-1}$, inverting yields $\rho = X/r$ or $\rho = \rho_0(X/X_0)^2$, where ρ_0 is the density at grammage X_0. For an exponential density profile, $\rho \propto e^{-z/h}$, where h is the atmospheric scale height, the dependence is linear with grammage: $\rho = X/h$. For small values of X (i.e., $X < X_c \equiv X_0^2/\rho_0 h$) the wind will always have a smaller density at a given grammage than the exponential. Since $\rho_0 \approx X_0/R$ in the wind, and $h \ll R$, we conclude that if ρ_0 is characteristic of a beam-induced wind and h is characteristic of an undisturbed stellar atmosphere, $X_0 \ll X_c$, and thus the densities are lower in the wind than in an undisturbed stellar atmosphere.

There is, however, considerable uncertainty in what the equilibrium density distribution actually will be. This leads to a corresponding uncertainty in the neutrino spectrum produced along each chord. For this reason, rather than using the neutrino spectrum calculated separately for each chord in an undisturbed companion, we have simply calculated the energy deposition that would result from the two extreme spectra in Figure 3. The $b = 0$ spectrum for the 2.8 $M_\odot$ case gives the lower limit because production of high-energy neutrinos is maximally supressed when the density of the region in which the neutrinos are produced is maximized. Correspondingly, the $b \approx R$ spectrum gives an upper limit to the neutrino energy deposition because the cascade takes place along the low-density edge of the companion where charged pions of all energies decay to give neutrinos. The $b \approx R$ spectrum will give the closest approximation to the neutrino spectrum which would be produced if the heating of the atmosphere drives a wind and the densities are lower than those in the normal stellar atmosphere.

IV. NEUTRINO ENERGY DEPOSITION

The dominant process for interaction of the ν_μ's produced when charged pions decay is the charged current mode:

$$\nu_\mu + N \rightarrow \mu + \text{hadrons} . \quad (8)$$

The cross section for this process rises linearly with neutrino energy until the 10–100 TeV range, after which it increases logarithmically (e.g., Stecker 1979). The corresponding interaction length (averaged over neutrinos and antineutrinos) is shown in Figure 4. The mean thickness of a 2.8 $M_\odot$ companion star is $\sim 2 \times 10^{11}$ g cm^{-2}, which is equal to the neutrino interaction length for neutrino energy ~ 2 TeV. Most neutrinos above this energy will be absorbed. Since the critical energy below which neutrinos will be produced by pion decay in the outer part of the star is $\gg 2$ TeV, we expect absorption of neutrino energy deep in the star to be important. Because of the high density of the region in which most neutrinos interact, their energy deposition will be fairly localized relative to the point of absorption, even for that part of the energy that goes into muons. Charged pions will interact and dissipate energy by cascading rather than decaying. High-energy neutral pions will decay to high-energy photons, which will produce electromagnetic cascades. Thus, virtually all the energy of neutrinos that interact will be in the form of low-energy photons heating the interior of the star.

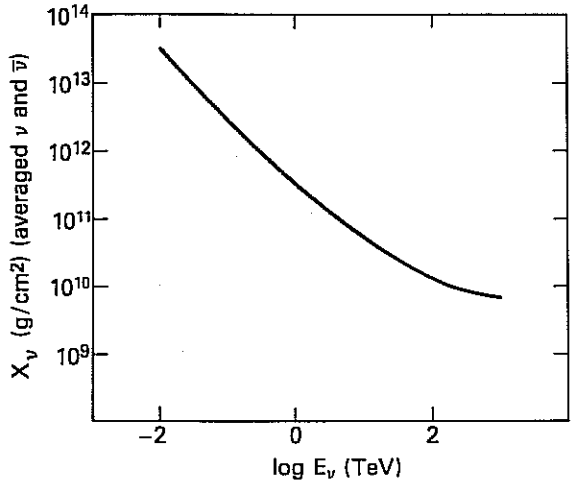

FIG. 4.—Neutrino interaction length X_ν(g cm^{-2}) vs. E_ν(TeV)

Using the standard stellar atmosphere profiles and taking account of pion cascading, we have numerically calculated the neutrino energy deposition, $\eta_\nu = fL_\nu$, as a function of a/R for two examples, the 2.8 $M_\odot$ example referred to above and a main-sequence star of 15 $M_\odot$. Table 2 displays the results as a fraction of the cosmic-ray power that is deposited in the companion by high-energy neutrinos for the two extreme production spectra calculated at $b = 0$ (soft) and at $b \approx R$ (hard). Here L_ν is the total produced neutrino luminosity and f is the fraction of the neutrino power that is absorbed in the companion. Thus, the quantity tabulated is η_ν/L_{cr}.

We may estimate this fraction as follows:

$$\frac{\eta_\nu}{L_{cr}} \approx \left[\!\!\left[\frac{1}{2}\left\{1 - \left[1 - \left(\frac{R}{a}\right)^2\right]^{1/2}\right\} \right]\!\!\right] \epsilon[1 - \exp(-\tau_\nu)] . \quad (9)$$

Here the quantity in double brackets is the fraction of the solid angle of the isotropic cosmic-ray source subtended by the companion star (and is $\propto [R/a]^2$ for $a/R \leq 3$), ϵ is the efficiency of converting incident beam energy into neutrino energy, and τ_ν is the optical depth of the star to neutrino absorption for those neutrinos carrying most of the energy. The optical depth of the star to neutrinos, τ_ν, is given approximately by

$$\tau_\nu(E_\nu, M) \approx \frac{1}{m_H}\sigma(E_\nu)\int \rho dr \approx 0.5\sigma(E_\nu)\frac{M}{m_H R^2} . \quad (10)$$

For neutrino energies below 10 TeV, $\sigma(E_\nu)$ is in the linear regime (e.g., Stecker 1979). This cross section, averaged over neutrinos and antineutrinos, is approximately given by $\sigma(E_\nu) \approx 5 \times 10^{-36} E_\nu(\text{TeV})$ cm^2 (see Fig. 4). For intermediate-mass main-sequence stars $R \approx R_\odot(M/M_\odot)^{0.63}$ so that equation (10) becomes

$$\tau_\nu(E_\nu, M) \approx 0.66 E_\nu(\text{TeV})(M/M_\odot)^{-0.26} . \quad (11)$$

For neutrinos produced by pions of energy $\sim E_\pi^c$ in the $b = 0$ case, as given by equation (2), τ_ν in equation (11) can be esti-

TABLE 2

NEUTRINO ENERGY DEPOSITION IN THE COMPANION STAR

	2.8 $M_\odot$		15 $M_\odot$	
a/R	$b \approx 0$	$b \approx R$	$b \approx 0$	$b \approx R$
1.1.....	0.0078	0.040	0.011	0.058
1.2.....	0.0064	0.033	0.0088	0.046
1.6.....	0.0035	0.017	0.0047	0.024
2.0.....	0.0022	0.011	0.0035	0.015
3.0.....	0.00098	0.0047	0.0013	0.0063

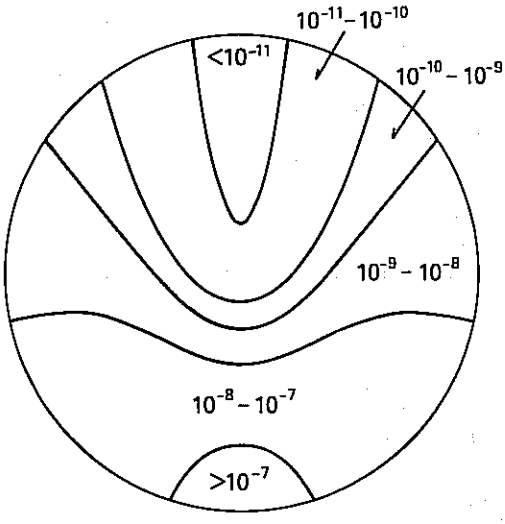

FIG. 5a

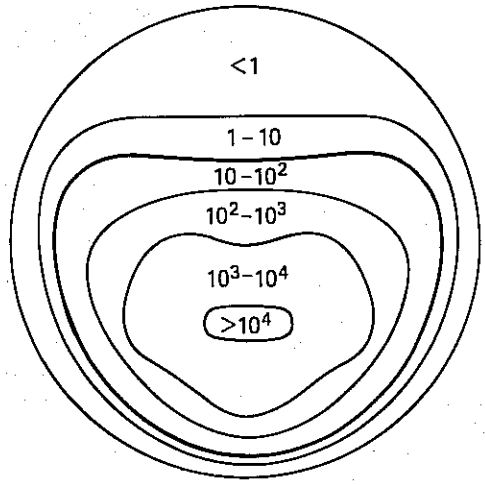

FIG. 5b

FIG. 5.—(*a*) Contour map of energy deposition per particle (eV per nucleon per second) for $M = 2.8\,M_\odot$, $a/R = 1.2$, and a $b = 0$ neutrino spectrum. The compact object is at the bottom of the figure. (*b*) Contour map of energy deposition per unit volume (ergs $\text{cm}^{-3}\,\text{s}^{-1}$) for $M = 2.8\,M_\odot$, $a/R = 1.2$, and the $b = 0$ neutrino spectrum.

mated once ρ is known at a depth of one pion mean free path $X \approx 30$ g cm^{-2}. For an exponential atmosphere $\rho = X/h$, where $h \approx kT/mg$ is the scale height, and $g = GM/R^2$. For intermediate-mass main-sequence stars the luminosity $L \approx L_\odot(M/M_\odot)^{3.9}$, so that $T \approx (L/4\pi R^2\sigma)^{1/4} \approx T_\odot(M/M_\odot)^{0.66}$. Thus $h \approx 1.73 \times 10^7(M/M_\odot)^{0.92}$ cm, yielding $\rho(X = 30\ \text{g cm}^{-2}) = 1.7 \times 10^{-6}(M/M_\odot)^{-0.92}$ g cm^{-3}. Substituting this into equation (2) gives $E_\nu^c \approx 0.67(M/M_\odot)^{0.92}$ TeV. Thus,

$$\tau_\nu^c \approx 0.44(M/M_\odot)^{0.66}\ . \tag{12}$$

For the $b = 0$ spectrum, $\tau_\nu^c > 1$ for a 15 $M_\odot$ star and is ~ 0.87 for a 2.8 $M_\odot$ star.

For the $b \approx R$ spectrum the optical depth will be much greater than 1. A numerical calculation of the details of the cascading process is required to determine ϵ. Data on the dynamics of high-energy collisions and simple kinematic considerations of pion decay lead to an estimate of $\epsilon \lesssim \frac{1}{4}$ in the $b \approx R$ case. Use of equation (9) and Table 2 indeed gives $\epsilon \approx 0.14$–0.22 for the $b = R$ case, while giving $\epsilon \approx 0.04$–0.06 for the $b = 0$ case (where we have used $\tau_\nu = 0.87$ for $M = 2.8\,M_\odot$ and $b = R$, $\tau_\nu \gg 1$ for the other cases). This discussion serves to supplement analytically the numerical results given for the specific cases considered here so that one may interpolate to other cases.

Figures 5 and 6 are contour maps of the localized energy deposition for our two examples for particular values of a/R. In

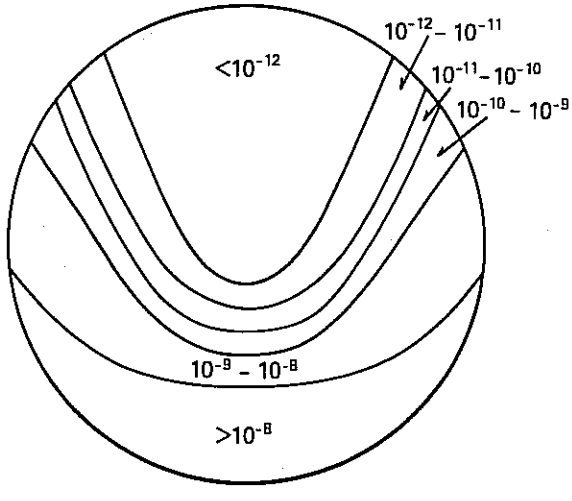

FIG. 6a

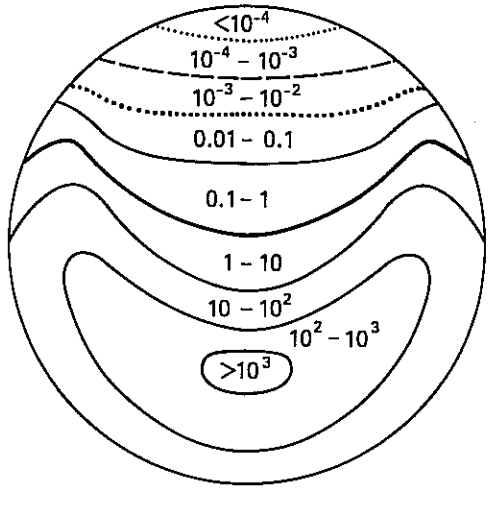

FIG. 6b

FIG. 6.—(*a*) Same as Fig. 5*a* for $M = 15\,M_\odot$, $a/R = 2$, and a $b \approx R$ spectrum. (*b*) Same as Fig. 5*b* for $M = 15\,M_\odot$, $a/R = 2$, and a $b \approx R$ spectrum.

Figure 5 (2.8 $M_\odot$) we show results for the $b = 0$ neutrino production spectrum, and in Figure 6 (15 $M_\odot$) we show the $b \approx R$ production spectrum. In both cases, as well as in Figure 3, the primary cosmic-ray spectrum was assumed to be a δ-function with $E = 10^8$ GeV.

V. EFFECTS OF NEUTRINO HEATING

There are at least two relevant quantities to which η_ν should be compared, viz., the Eddington luminosity, L_E, and the stellar luminosity, L, due to nucleosynthesis. If the neutrino energy deposition rate exceeds L_E the whole system may be disrupted. If η_ν is less than L_E but greater than L the system may be modified substantially in a time shorter than the lifetime of the system as estimated from the observed orbital period derivative. SHB suggested that the companion may expand in response to the neutrino heating and quench the accelerator. We now discuss these possibilities in greater detail, in light of the more accurate estimates of neutrino energy deposition given in the preceding section.

If the companion star can absorb a significant fraction of its binding energy, it will alter its structure. The time to absorb a binding energy, $E_B \approx GM^2/R$, at a rate equal to the heating by neutrinos is

$$t_B = \frac{E_B}{\eta_\nu} \approx 10^3 \text{ yr} \left(\frac{M}{M_\odot}\right)\left(\frac{R_\odot}{R}\right)\left(\frac{L_E}{\eta_\nu}\right), \quad (13)$$

at which point the star will be completely disrupted. For heating rates near the Eddington limit, this time is relatively short.

If the neutrino heating rate in the interior of the star exceeds the intrinsic stellar luminosity, the central temperature will initially increase. The star will adjust to restore hydrostatic equilibrium, reducing the central temperature, on a dynamic time scale, $t_D = 1/(G\rho)^{1/2} \approx 1$ hr, which is short compared to t_B. In a dynamic time scale, the central temperature will increase by only a small fraction,

$$\frac{\delta T}{T} \approx \frac{t_D}{2t_B} = 2.7 \times 10^{-8}\left(\frac{R}{R_\odot}\right)^{5/2}\left(\frac{M}{M_\odot}\right)^{-3/2}\left(\frac{\eta_\nu}{L_E}\right) \quad (14)$$

of the initial temperature. Even though the nuclear reaction rates in the core are a sensitive function of temperature, their resulting increase will not be large enough to cause a thermal runaway. Instead, the star will expand on a relatively slower time scale, t_B, maintaining quasi-hydrostatic equilibrium. As it expands, the central temperature drops, the radiative cooling at the surface increases (as a result of the larger surface area), and the entire star actually cools as a result of the extra heating. From the virial theorem and energy conservation, one can show that the initial behavior of the radius of the star as a function of time during which continuous heating $\eta_\nu > L$ occurs is

$$R(t) \approx R_0/(1 - t/t_0), \quad t < t_0, \quad (15)$$

where the constant $t_0 = (GM^2/R_0)/\delta L$, $\delta L = \eta_\nu - L$, and R_0 is the initial radius of the star. This equation assumes that all of the absorbed energy goes into work against gravity in expanding the star, which is a good approximation until the photon diffusion time becomes comparable to t_0. At this point, the star begins to lose some energy through radiative cooling from the surface, and the expansion will slow down (unless $\eta_\nu > L_E$). As the companion star expands it will become somewhat more transparent to neutrinos than the initial "undisturbed" star for which the absorption calculations were done. Thus, the characteristic time would be somewhat longer than the estimates in equations (13) and (15), but not significantly so for close binaries. Even for heating rates substantially below L_E, the companion star radius in a close binary could increase enough to exceed the orbital radius and engulf the compact object. We speculate that this could lead to a mechanism for periodically turning the accelerator on and off which might lead to various observable effects in addition to modulation of the high-energy signal, such as pulsations, radio outbursts, X-ray outbursts, etc.

For Hercules X-1 and possibly Cygnus X-3, the 2.8 $M_\odot$ example is the relevant one, whereas for LMC X-4 and Vela X-1 the companion mass is somewhat above 15 $M_\odot$. In the first case $L_E \approx 3 \times 10^{38}$ ergs s^{-1} and $L \approx 10^{35}$ ergs s^{-1}, and in the second the corresponding numbers are 10^{39} and 10^{38} ergs s^{-1}. We now use information from Tables 1 and 2 to make the comparison with the neutrino energy deposition. For Vela X-1 the separation is so great and the companion so massive that $\eta_\nu \ll L$. For Hercules X-1, $\eta_\nu \approx L$. The other two cases are the most interesting because in both cases the neutrino energy deposition is substantially greater than the stellar luminosity. For the 2.8 $M_\odot$ case, we estimate $\eta_\nu \approx 10^{37}$ ergs s^{-1} for the neutrino heating rate, and the expansion time scale $t_0 \approx t_B = 3.8 \times 10^4$ yr. From equation (15), it follows that the time for the star to expand to the radius of the orbit when $a/R_0 = 1.2$ is $t = 6.3 \times 10^3$ yr. In the 15 $M_\odot$ (LMC X-4) case, we estimate a heating rate of $\eta_\nu \approx 3 \times 10^{38}$ ergs s^{-1}, giving $t_0 = 6.2 \times 10^3$ yr and $t = 4.4 \times 10^3$ yr for $a/R_0 = 3.5$.

Several possible scenarios may follow the neutrino-heating induced expansion of the companion star. If the acceleration mechanism is quenched when the compact object is engulfed in the atmosphere of the companion, then neutrino production and heating will cease, and the star will begin to contract. Once the companion has contracted within the radius of the orbit, the acceleration might resume, and some kind of periodic behavior may result. The period would be no longer than t_0, the time scale on which stellar radius changes occur, which is probably too long to be observable in the Cygnus X-3 and LMC X-4 systems. (The lower limit on the period is $\sim t_D$). But if this periodic turning on and off of the acceleration adjusts itself so that the time-averaged heating of the star is approximately equal to L (if the stellar luminosity is governed by a mass-luminosity relation), then the fraction of time during which acceleration is on will be $f_{on} = L/\eta_\nu \approx 10^{-2}$ for the Cygnus X-3 case. The interval of time during which the source is turned on in a period t_0 is then $f_{on} t_0 \lesssim 100$ yr. If the oscillation period is between t_D and several years, the γ-ray observations would indicate an average luminosity of the star to be a few percent of $\sim 10^{39}$ ergs s^{-1}. This is larger than what is expected for an intermediate-mass main-sequence star.

If the accelerator does not turn off inside the envelope of the companion star, then the heating and expansion of the star will continue. On a time scale t_0, the stellar material surrounding the compact object will become optically thick, first to the X-rays (depth of ~ 1 g cm^{-2}) and then to the γ-rays (depth of ~ 50 g cm^{-2}). This time scale may be shortened by the orbital decay due to frictional dissipation in the stellar atmosphere (Taam, Bodenheimer, and Ostriker 1978). Thus, this scenario is ruled out, unless we should happen to be observing the system during its first 10^3–10^4 yr.

Should the compact object then fall to the center of the companion star and somehow continue to accelerate high-

energy particles, it is amusing to speculate that a "hidden neutrino source" (Berezinsky 1980) might result, but here again the stellar atmosphere would continue to expand and be blown off. Needless to say, in this "swallowed star" configuration, no significant γ-ray flux or time-variable neutrino flux would be expected, so that this case does not refer to any of the real observed systems which are the main concern of this paper.

Since no optical emission has been seen from the companion in the Cygnus X-3 system, its mass is very uncertain, in contrast to the other ultra-high-energy binaries whose companions have been detected optically. Requiring the companion to be a main-sequence star with a radius less than the orbital radius gives a mass upper limit of 4 $M_\odot$ (Vestrand and Eichler 1982). Requiring the star to fit inside its own Roche lobe gives an upper limit of 0.5 $M_\odot$ for a main-sequence star (Patterson 1984) but could be several $M_\odot$ for a He star (van den Heuvel and de Loore 1973). Although we have presented detailed calculations of the neutrino heating rate for the case of a 2.8 $M_\odot$ companion, we may use equations (9) and (13) to get an estimate of the heating rate and lifetime of the system for other values of the companion mass. The time for a star of mass M to absorb its binding energy in neutrinos is

$$t_B \approx 10^3 \text{ yr} f\left(\frac{M}{M_\odot}\right)\left(\frac{0.2}{\epsilon}\right)L_{39}^{-1}, \quad (16)$$

where the function $f(M/M_\odot)$ involves the mass-radius relation for main-sequence stars as well as the geometrical and optical depth factors, and $L_{39} = (L_{cr}/10^{39} \text{ ergs s}^{-1})$. This time scale is plotted as a function of mass in Figure 7 for the two extreme neutrino production spectra. The break around 1.3 $M_\odot$ results from a corresponding break in the particular mass-radius relation which we have used (Lacy 1977). The lifetime of a 0.5 $M_\odot$ star lies between $\sim 10^4$ and $\sim 10^5$ yr, with the lower value applicable to a star with a dense wind (see § III) and the higher value being an upper limit. This lifetime is a very small fraction of the main-sequence lifetime of a 0.5 $M_\odot$ star and is not significantly different from that derived for the 2.8 $M_\odot$ star.

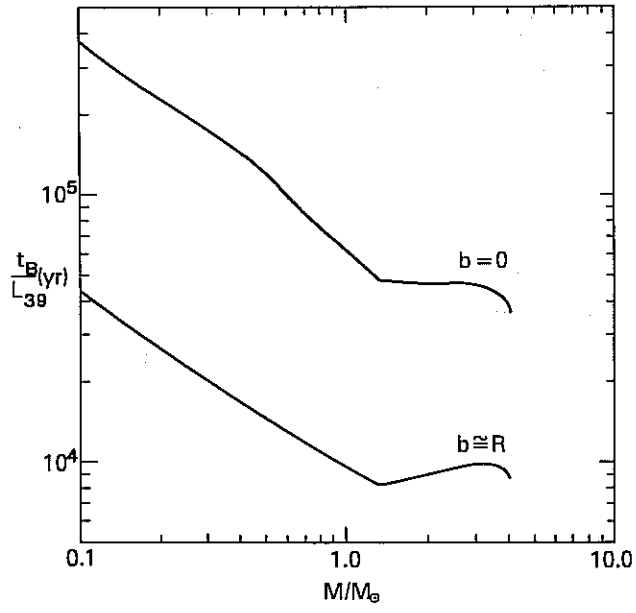

FIG. 7.—Lifetime of a main-sequence companion star against disruption by neutrino heating in the Cygnus X-3 system, scaled by the incident proton luminosity $L_{39} = L_{cr}/10^{39}$ ergs s^{-1}, as a function of its mass from eq. (16). Upper and lower curves were determined for the two extreme neutrino spectra produced at impact parameters $b = 0$ and $b \approx R$. Values of 0.20 and 0.05 were used for the neutrino production efficiency ϵ in the $b \approx R$ and $b = 0$ cases, respectively. The mass-radius relation for main-sequence stars is that given by Lacy (1977).

Finally, we note that in the case of Cygnus X-3, η_ν could be as much as 1.5 orders of magnitude larger without completely disrupting the system. For LMC X-4 it could be a factor of 3 or so larger. Thus, the neutrino-induced signal could be as large as 10–30/1000 m^2 yr^{-1}, rather than the more conservative estimate of $\sim$one per year in 1000 m^2. This would require D_γ in equation (1) to be much smaller than 1/50. However, this duty factor for production of photons is very model dependent because of the narrow range of thicknesses for which high-energy photons can be produced without being reabsorbed. A flux as large as this limiting value would still not be large enough to explain the reported underground signals from the direction of Cygnus X-3 observed with exposures of ~ 10 m^2 yr (Marshak *et al.* 1985; Battistoni *et al.* 1985); however, it could be detectable in the large area detector proposed for Grand Sasso (the MACRO collaboration 1985) and certainly in a detector with an area as large as 10^5 m^2 as proposed for DUMAND (Roberts 1979).

Several factors may influence the above constraints imposed by neutrino heating of the companion star. We have assumed that the accelerated particles are emitted isotropically. If the cosmic rays from the source are sufficiently anisotropic, then neutrinos would not heat the entire volume of the companion star. While there are no direct constraints on the solid angle of the particle beam in any of the ultra–high-energy γ-ray sources, in the case of Cygnus X-3 constraints on the mass loss from the companion star may indicate that the beam heats a small fraction of the stellar surface area (SHB). However, as long as the total energy incident on the star remains the same, we do not expect, given the near uniform energy deposition over the star (see Figs. 5 and 6), that the neutrino absorption will change significantly. There is also evidence that Cygnus X-3 is a highly variable source at high energies on a time scale of $\ll 100$ yr (Bhat *et al.* 1985), which would ease the energy constraints on the system, since our limits refer to time-averaged energy constraints over time scale of 100 yr or more.

VI. CONCLUSION

We have examined close binary star models for ultra–high-energy γ-ray sources in which primary cosmic rays accelerated by a compact object interact with the companion star. We have shown that significant amounts of energy are deposited deep in the star by neutrinos produced along with the ultra–high-energy γ-rays as a result of cosmic-ray pion production and decay. This energy deposition was shown to have dramatic effects on the evolution of some binary systems. For the Cygnus X-3 and LMC X-4 systems in particular, our calculated neutrino heating rate exceeds the intrinsic stellar luminosity, changing the internal structure of the companion star. We estimate that these systems will evolve or change their characteristics on time scales of 10^3–10^4 yr. Thus, we are either fortunate enough to be observing these sources during their relatively short lifetimes, or they are highly time variable, or the companion star is not the site of the observed ultra–high-energy γ-ray production. There may be some support for the latter two alternatives in the case of Cygnus X-3 which is highly time variable (e.g. Bhat *et al.* 1985) and where recent

observations indicate that the phase of maximum photon production is ~0.6 (Watson 1986). Since this is roughly the phase of maximum X-ray flux, it would seem to indicate that the compact star is in front of, rather than behind, the companion star at these times.

In accordance with SHB, we conclude that high-energy neutrino interactions can play a major role in determining the evolution of close X-ray binaries in which a compact object is a powerful source of ultra–high-energy cosmic rays that impinge on a companion star. Thus, the general neutrino physics constraints on these systems (derived here for particular examples), in conjunction with future observations of ultrahigh energy γ-rays and underground muons and neutrinos from such systems, can be used to study the (possibly pathological) structure and evolution of the companion star as well as the characteristics of the "pevatron" accelerator associated with the compact object.

We are grateful to David Eichler, John Faulkner, Demosthenes Kazanas, and Shmuel Nussinov for helpful discussions. Work of T. K. G. is supported in part by NSF and DOE under DE-AC02-78E8-05007.

REFERENCES

Baltrusaitis, R. M., *et al.* 1984, *Phys. Rev. Letters*, **52**, 1380.
———. 1985, *Ap. J. (Letters)*, **293**, L69.
Barnhill, M. V., III, Gaisser, T. K., Stanev, T., and Halzen, F. 1985, *Nature*, **317**, 409.
Battistoni, G., *et al.* 1985, *Phys. Letters*, **155B**, 465.
Baym, G., Kolb, E. W., McLerran, L., and Walker, T. P. 1985, *Phys. Letters*, **160B**, 181.
Bayere, P., *et al.* 1985, *Proc. 19th Internat. Cosmic Ray Conf.*, **9**, 465.
Berezinsky, V. S. 1980, in *Proc. 1979 DUMAND Summer Workshop*, ed. J. G. Learned (Honolulu: University of Hawaii Press), p. 245.
———. 1985, *Proc. 19th Internat. Cosmic Ray Conf.*, **1**, 75.
Bhat, C. L., *et al.* 1985, *Proc. 19th Internat. Cosmic Ray Conf.*, **1**, 83.
Chadwick, P. M., *et al.* 1985, *Nature*, **318**, 642.
Chudakov, A. E. 1985, *Proc. 19th Internat. Cosmic Ray Conf.*, **9**, 441.
Eichler, D. 1978, *Nature*, **275**, 725.
Gaisser, T. K., and Stanev, T. 1985, *Phys. Rev. Letters*, **54**, 2265.
Hillas, A. M. 1984, *Nature*, **312**, 50.
Kifune, T., *et al.* 1985, *Proc. 19th Internat. Cosmic Ray Conf.*, **1**, 67.
Lacy, C. H. 1977, *Ap. J. Suppl.*, **34**, 479.
Lloyd-Evans, J., *et al.* 1983, *Nature*, **305**, 784.
Marshak, M. L., *et al.* 1985, *Phys. Rev. Letters*, **54**, 2079.
Mackenzie, P. B., and Thacker, H. B. 1985, *Phys. Rev. Letters*, **55**, 2539.
MACRO collaboration. 1985, *Proc. 19th Internat. Cosmic Ray Conf.*, **8**, 136.
Mohapatra, R. N., Nussinov, S., and Vallé, J. W. F. 1985, *Phys. Letters*, **165B**, 417.
Patterson, J. 1984, *Ap. J. Suppl.*, **54**, 443.
Protheroe, R. J., and Clay, R. W. 1985, *Nature*, **315**, 205.
Protheroe, R. J., Clay, R. W., and Gerhardy, P. R. 1984, *Ap. J. (Letters)*, **280**, L47.
Rappaport, S. A., and Joss, P. C. 1983, in *Accretion-driven Stellar X-Ray Sources*, ed. W. H. G. Lewin and E. P. J. Van den Heuvel (Cambridge: Cambridge University Press), p. 1.
Roberts, A., ed. 1979, *Proc. 1978 Internat. DUMAND Symposium*, Vols. 1, 2 (La Jolla: Scrips Institution of Oceanography).
Samorski, M., and Stamm, W. 1983*a*, *Ap. J. (Letters)*, **248**, L17.
———. 1983*b*, *Proc. 19th Internat. Cosmic Ray Conf.*, **11**, 244.
Stecker, F. W. 1979, *Ap. J.*, **228**, 919.
Stecker, F. W., Harding, A. K., and Barnard, J. J. 1985, *Nature*, **316**, 418 (SHB).
Stenger, V. 1985, *Nature*, **317**, 411.
Taam, R. E., Bodenheimer, P., and Ostriker, J. P. 1978, *Ap. J.*, **222**, 260.
van den Heuvel, E. P. J., and de Loore, C. 1973, *Astr. Ap.*, **25**, 387.
Vestrand, W. T., and Eichler, D. 1979, in *Proc. AIP Conf. 56, Particle Acceleration in Astrophysics*, ed. J. Arons, C. McKee, and C. Max (New York: AIP), p. 285.
———. 1982, *Ap. J.*, **261**, 251.
Watson, A. A. 1986, *Proc. 19th Internat. Cosmic Ray Conf.*, in press.

J. J. Barnard, A. K. Harding, and F. W. Stecker: Code 665, Laboratory for High Energy Astrophysics, NASA/Goddard Space Flight Center, Greenbelt, MD 20771

T. K. Gaisser: Bartol Research Foundation, University of Delaware, Newark, DE 19716